

Advanced lasers for photonic device microfabrication

Peter R. Herman,^{*1} Kevin P. Chen,^{*1} Paul Corkum,^{*2} Andrei Naumov,^{*2} Sandy Ng,^{*1}, and Jie Zhang^{*1}

^{*1} *Department of Electrical and Computer Engineering, University of Toronto, Canada*

^{*2} *Steacie Institute for Molecular Sciences, National Research Council of Canada, Canada*

Today's internet-focused communication industry is driving a powerful transition from slower electronic systems to high-speed all-optical systems. A central effort is the miniaturization and integration of photonic devices into highly functional optical circuits. New processing and packaging technologies are now required that can precisely shape and assemble optical components to sub-wavelength accuracy – an area that laser microfabrication technology can potentially serve. However, applications are restricted only to lasers providing strong interactions with *transparent* optical materials. Our groups are exploring two extremes in laser technology – ultrafast lasers and short-wavelength F₂ lasers – to microsculpt optical surfaces and to profile refractive-index structures inside transparent glasses. This report offers head-to-head comparisons of photosensitivity responses (refractive index change), spatial resolution, and processing windows for the deep-ultraviolet and ultrafast lasers, and discusses prospects for laser printing and trimming of optical waveguide components and circuits.

1. Introduction

High-speed photonics is now the critical enabling technology providing ever-increasing bandwidth for the Internet-driven communications industry. At the forefront, is the race to develop new processing and packaging technologies that can miniaturize and integrate optical devices into highly functional optical circuits, an effort analogous with the miniaturization and integration of electronic components onto semiconductor chips more than four decades earlier. Laser microfabrication technology can play a significant role here much in the way lasers are currently applied in lithography, trimming, repair, and inspection of today's semiconductor electronic chips. For photonic devices, applications are restricted to advanced laser sources that interact strongly with transparent materials. To this end, our groups are exploring two extreme laser approaches to shaping structures in glasses: ultrafast (UF) and deep-ultraviolet (UV) laser processing.

One potential approach to photonic component manufacturing is laser ablative micromachining. Our University of Toronto groups have provided head-to-head comparisons of UV F₂-laser and UF (1 ps) laser approaches, and introduced a new UF-laser processing mode called *burst machining*.^{1,2} Delivered fluence was key to driving strong absorption mechanisms that permit smooth sculpting of surfaces by coupling sufficient energy per unit volume to heat, melt, and ablate fused silica irrespective of absorption channels.

In a further extension of this micromachining effort, our groups have applied ultrafast and F₂ lasers to drive more subtle interactions to control and to profile refractive-index change internally in optical glasses.^{1,3} The present paper summarizes our findings by comparing processing rates for far UV and UF lasers in processing glass materials. We compare photosensitivity responses, spatial resolution, and processing windows, and discuss prospects for printing and trimming optical waveguides and circuits. Accumulated fluence is found to control to the magnitude of the induced refractive-index change. There also appears a possible thermal role for UF processing that enhances photosensitivity responses for repetition rates ≥ 10 kHz; an analogous *burst machining* effect was described previously^{1,2} that provides crack-free ablation

of transparent glasses.

2. Photosensitivity background

Refractive-index profiling of fiber Bragg and long-period gratings with traditional ultraviolet lasers (193, 248 nm)^{4,5} is of current commercial importance to the photonics industry. Interest is also developing in trimming optical components, for example, to correct phase errors in arrayed waveguide gratings.^{6,7} For these waveguide applications, photosensitivity enhancement techniques are normally required to speed processing times and to increase the absolute value of laser-induced refractive-index change.⁴ Our group has examined the extension of such techniques to record short-wavelength light from the F₂ laser. The 157-nm photons offer faster and stronger photosensitivity responses without the need for an enhancement technique.^{1,8} Strong linear interactions near the optical bandedge of both germanosilicate and pure silica glasses provide useful refractive-index changes in the range of $\sim 10^{-4}$ to $> 10^{-3}$. For pure fused silica, the photosensitivity response is found to be orders-of-magnitude more rapid than with that provided by traditional UV lasers (193 or 248 nm).^{9,10}

UF lasers drive fundamentally different interactions that lead also to useful refractive index changes in transparent glasses.^{3,11–13} We describe optical waveguides formed with 50-fs pulses of 800-nm light at 1–100 kHz repetition rates, a sharp contrast to the 15-ns duration and 100-Hz rates of the 157-nm F₂ laser. UF laser-matter interaction dynamics is not fully understood. As in UV-laser induced index changes (compaction, color centers^{4,5}), there are several proposed contributing factors, for example, multiphoton ionization, field ionization, electron avalanche, *microexplosion*,¹¹ compaction, and color centers.¹⁰

3. Experiments

A commercial F₂ laser (Lambda Physik, LPF220i) provided 157-nm light pulses of ~ 20 -mJ energy and ~ 15 -ns duration at 100-Hz repetition rate. Apertures and lenses were applied

to the $20 \times 7\text{-mm}^2$ beam ($\sim 3\text{-mrad}$ by $\sim 1\text{-mrad}$ divergence) to provide uniform exposure and to control fluence. A sealed processing chamber was flushed with 1-atm argon gas for vacuum-ultraviolet transparency.

The UF laser consisted of an Ar^+ -pumped Ti:sapphire oscillator, a stretcher, a regenerative amplifier (Coherent RegA 9050), and a single-grating compressor. The 800-nm laser provided $1.5\text{-}\mu\text{J}$ energy in 50-fs pulses at repetition rates variable up to 250 kHz. The beam was focused into glass samples to a $3\text{-}\mu\text{m}$ diameter with a 10X microscope objective and scanned along the optical axis with $0.1\text{-}\mu\text{m}$ step-size stepper motors.

The samples consisted of UV-grade fused silica cover slips and windows (Corning 7940), polished fused silica blanks, 3% GeO_2 -doped planar waveguides (PIRI SMPWL) and single-mode optical fibers (SMF28). Laser-induced refractive index changes were assessed by various techniques as described below.

4. Photosensitivity responses

4.1 Fused silica with 157-nm radiation

The F_2 laser was directly applied to fused silica glasses through a proximity amplitude mask of $140\text{-}\mu\text{m}$ period to form volume gratings. Figure 1 shows a side view of the refractive-index contrast induced inside a 2-mm thick polished window (Corning 7940; 1,200 ppm OH) with 180,000 pulses at $\sim 84\text{ mJ/cm}^2$ fluence. A $\sim 1\text{-mm}$ grating depth was formed, matching approximately the penetration depth associated with the 157-nm absorption coefficient of $\alpha_{157} \sim 10\text{ cm}^{-1}$.

To characterize refractive index changes, wet-fused silica (OH: 1,200 ppm; $\alpha_{157} = 26\text{ cm}^{-1}$) cover slips of thickness $d = 0.16\text{ mm}$ were radiated with 157-nm light. A first-order diffraction efficiency of 0.1 to 1.5% was measured with a HeNe laser for samples exposed to $F = 51, 70,$ and 84 mJ/cm^2 fluence and pulse number in the $N = 60,000\text{--}360,000$ range. Several samples were stacked together during one exposure, and a numerical model of exponential index profile, $\Delta n e^{-\alpha d}$, yielded an effective absorption coefficient of $\alpha = 26\text{ cm}^{-1}$.

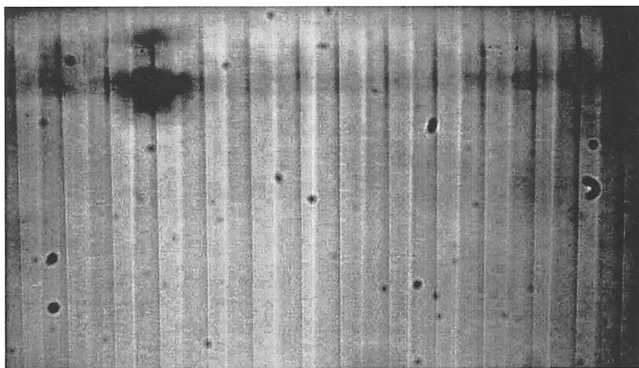


Fig. 1. Optical microscope side view of a fused silica window after 157-nm laser exposure with 180,000 pulses at $\sim 84\text{ mJ/cm}^2$ fluence. A volume grating of $140\text{-}\mu\text{m}$ period was formed deep ($\sim 1\text{ mm}$) into the glass.

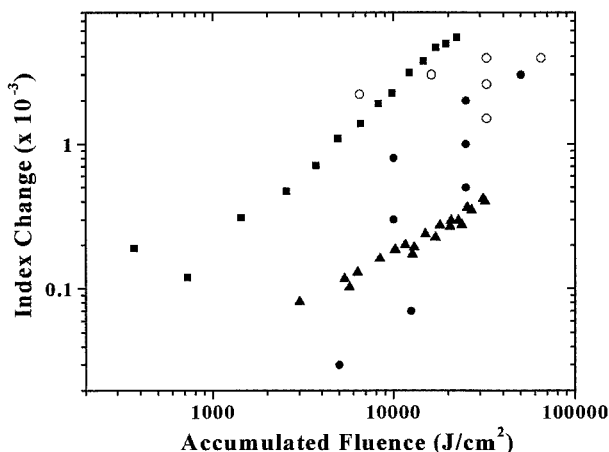


Fig. 2. Comparison of deep UV and UF laser induced index changes in fused silica and germanosilicate glasses: \blacktriangle F_2 -laser on pure fused silica, \blacksquare F_2 -laser on GeO_2 -doped (3%) fused silica, \circ UF-laser on fused silica (10–100 kHz), and \bullet UF-laser on fused silica (1 kHz) from.¹²⁾ See text for further details.

The surface index changes, Δn , are plotted in Fig. 2 as a function of NF . The clustering of the data about a single line shows that index changes are controlled by accumulated fluence, NF , for the present processing range. This simple response offers advantages in concentrating finite laser energy to increase fluence and processing speed, or reducing fluence for larger area exposure at slower rates.

The bulk refractive-index change was also accompanied by surface compaction on the scale of 10's of nm on laser-irradiated surfaces. Changes in absorption at 157 nm and in the near infrared are also noted with increasing laser exposure. At the surface, refractive-index changes (in Fig. 2) follow a universal material compaction response of $\Delta n \sim (NF)^{0.70}$, a single-photon response that greatly exceeds the two-photon volume compaction response of $\Delta \rho \sim (NF^2)^{0.53}$ reported^{9,10)} for 193-nm exposure of fused silica. Overall, 157-nm laser-induced compaction and refractive index changes are approximately three orders of magnitude faster than reported for 193- or 248-nm lasers.^{9,10)} For 157-nm laser radiation, an absolute index changes of 4.2×10^{-4} is available in an $\sim 400\text{-}\mu\text{m}$ thick surface layer after a 60-min exposure (at 100 Hz). Such index change can provide useful phase correction for a wide range of applications in shaping and trimming optical components made with pure silica.

4.2 Germanosilicate waveguides with 157-nm radiation

Germanium doping of fused silica provides a controlled increase in refractive index to define the waveguide cores of optical fibers and planar circuits. Such doping also lowers the bandgap from $\sim 9.1\text{ eV}$ of fused silica to values comparable with the 7.9-eV photon energy of the F_2 laser. This provides strong absorption in thin layers on scale lengths commensurate with telecommunication waveguide geometries of $\sim 10\text{ }\mu\text{m}$. The F_2 laser is therefore an ideal candidate for fabricating photonic components and circuits inside germanosilicate fiber and planar waveguides.^{1,8)}

Standard telecommunication fibers (SMF 28) and silica-based cladless planar waveguides (PIRI SMPWL) were exposed to 157-nm radiation. The planar waveguide consisted of $8\text{-}\mu\text{m}$ thick GeO_2 -doped (3%) core layer grown over $20\text{-}\mu\text{m}$ of fused

silica, all on a silicon substrate. Germanosilicate glasses are much more photosensitive ($> 10X$) than the fused silica cladding, dominating the contribution of measured refractive-index change.

Figure 2 shows the peak refractive-index change observed in planar waveguides as a function of accumulated laser fluence. The single-pulse fluence was $\sim 7.5 \text{ mJ/cm}^2$. Effective index values from three guiding modes were determined from prism-coupling angle changes using HeNe laser probe light. These values were applied to a simple step-profile model of refractive index,³⁾ with bulk index change (Fig. 2) and penetration depth as the only adjustable parameters. The inferred penetration depth decreased from $\sim 8 \mu\text{m}$ at low fluence to $\sim 4 \mu\text{m}$ for above 10-kJ/cm^2 fluence.

An unsaturated peak index change of 0.005 is obtained with only 22-kJ/cm^2 fluence. Hydrogen loading of the waveguide (105 bar for 10 days) provided a 3-fold faster response rate,³⁾ a modest improvement in comparison with order-of-magnitude enhancements seen with longer wavelength exposure.¹⁴⁾ Because of stronger absorption, the germanosilicate waveguides are an order of magnitude higher than for the case of pure fused silica. Further, this index change is strong and rapid compared with longer-wavelength exposure of similar germanosilicate waveguides (3% GeO_2) without H_2 -loading techniques. For example, responses are an order of magnitude faster than with 193-nm radiation, and follow a single-photon response in comparison with inferred two-photon responses.¹⁵⁾

A rapid 157-nm photosensitivity response was also found⁸⁾ for standard telecommunication fiber (Corning SMF-28). Figure 3 shows an optical microscope picture of coupled 633-nm HeNe-laser light scattering from a long-period grating ($140\text{-}\mu\text{m}$ period). The scattering light is mainly visible from one side of the fiber suggesting a non-uniform index-change profile similar to that inferred above for the multimode planar waveguide.

The transmission spectrum of a similar long-period fiber grating with $304\text{-}\mu\text{m}$ period is shown in Fig. 4 for the case of a H_2 -loaded sample (at 100 bar for 10 days). A $\sim 20\text{-dB}$ loss peak is noted at the $1.58\text{-}\mu\text{m}$ telecommunication band. This

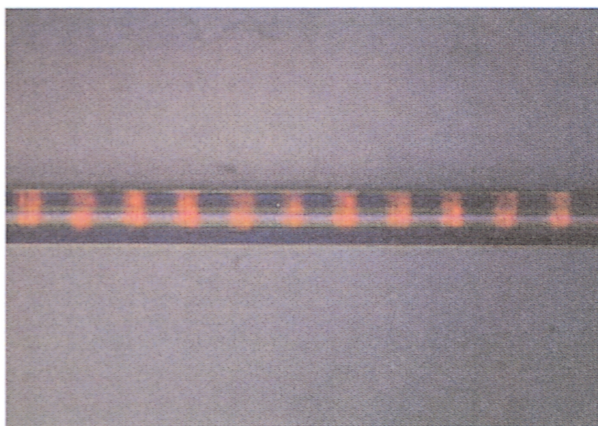


Fig. 3. HeNe-laser light scattered from long period grating ($\Lambda = 140\text{-}\mu\text{m}$) inscribed in a Corning SMF-28 fiber by the 157-nm F_2 laser.

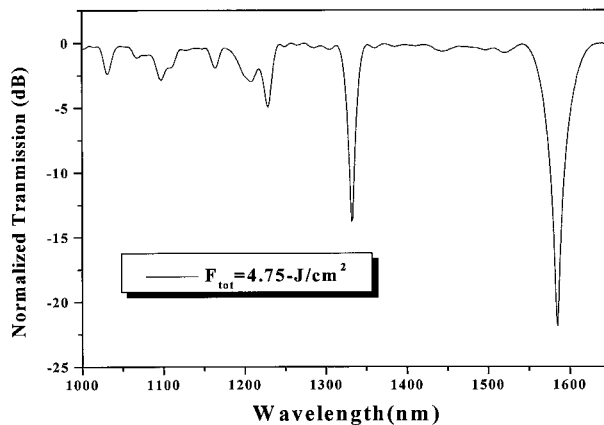


Fig. 4. Transmission spectrum of a long period grating ($\Lambda = 304\text{-}\mu\text{m}$) formed in hydrogen loaded SMF-28 fiber with the 157-nm F_2 laser.

response developed with 2,700 pulses at $\sim 1.8 \text{ mJ/cm}^2$ fluence – or with only $\sim 4.75\text{-J/cm}^2$ total fluence. For 248-nm KrF lasers, a $> 300\text{-fold}$ larger total fluence is required to develop the same strength loss peak. F_2 -laser radiation clearly drives strong material responses in germanosilicate glasses.

4.3 Fused silica with ultrafast lasers

UF-laser photosensitivity responses of fused silica were assessed by forming single-mode optical waveguides. Processing windows for low-loss waveguides were affected by pulse energy, repetition rate, scan speed, and focus diameter. Figure 5 shows over-exposed waveguides formed at 100 kHz and 10 kHz rates under similar fluence and accumulated fluence conditions. For 100 kHz repetition rate, there is noticeably more damage. Good quality waveguides were difficult to photograph.

Refractive-index changes were inferred from numerical aperture (NA) measurements (full-width half maximum) using

$$NA = \sqrt{2 \cdot n \cdot \Delta n}, \quad (1)$$

where n is the bulk glass index. Laser-diode light at 650 nm was coupled with 0.1-NA optics and detected at the waveguide output with a CCD camera through a 0.30-NA micro-

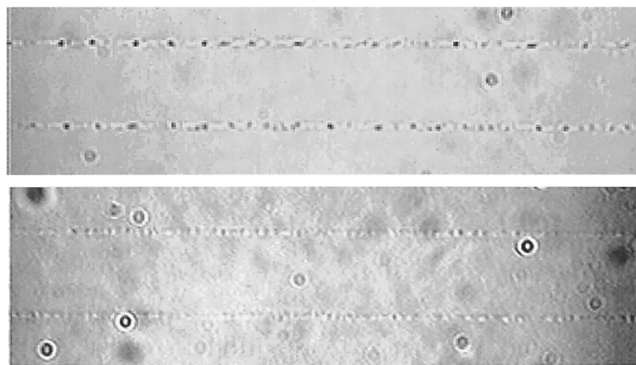


Fig. 5. CCD optical microscope image of waveguides written inside bulk fused silica by 100-kHz (top) and 10-kHz (bottom) repetition rate UF-laser pulses with $1\text{-}\mu\text{J}$ per pulse energy. Scan speeds were 200 and $20 \mu\text{m/s}$, respectively, to deliver identical accumulated fluence. Waveguides are spaced $50 \mu\text{m}$ apart.

scope objective at 32x magnification. A pinhole was located at the image plane to filter uncoupled laser light.

A maximum index change of $\sim 5 \times 10^{-3}$ was measurable, limited by heavy waveguide losses and poor coupling efficiency for waveguides damaged as shown in Fig. 5 (top). Weak waveguiding limited the measurement sensitivity to $\Delta n \sim 1 \times 10^{-3}$. This index range matches well the values typically seen in standard telecommunication fiber waveguides. Preliminary results of Δn are shown in Fig. 2 for 10- and 100-kHz repetition rates. Also shown for comparison purposes are index changes as reported by Gaeta and coworkers¹³⁾ using 100-fs pulses at 1-kHz repetition rate. Accumulated fluence was based on total exposure within one confocal beam parameter. Results fall into a similar range with the F₂-laser results, the accumulated fluence being key to the total achievable index change.

The 10- and 100-kHz UF laser data also suggest 2-fold or higher photosensitivity enhancement due to accumulative heating effects. The thermal diffusion scale length, L_{th} , for laser pulse separation time, t , is determined from

$$L_{th} = \sqrt{4 \cdot D \cdot t}, \quad (2)$$

where D is the thermal diffusion coefficient. For fused silica, this yields scale lengths of $6 \mu\text{m}$ and $60 \mu\text{m}$ for repetition rates of 100 kHz and 1 kHz, respectively. Comparison with the $\sim 3\text{-}\mu\text{m}$ focused diameter of the laser suggests that absorbed laser energy is not dissipated between pulses for the higher repetition rate case and accumulated heated effects may indeed enhance the refractive index change. We have reported similar heating effects in UF-laser burst machining of fused silica that appear responsible for microcrack elimination.^{1,2)} An accumulated heating effect also appears to underlie the *microexplosion* effect in Ref. 12.

5. Comparison between UV and UF processing

The 157-nm photon provides near bandedge absorption, very much like a single photon response. The UF interaction entails additional physical mechanisms – multi-photon ionization, field ionization, electron avalanche – to couple light into the transparent medium before phonon relaxation, thermal transport and other physical processes leave a permanent mark on the local refractive index. Surface and bulk studies verify both compaction and color center roles in the F₂-laser photosensitivity processes. Similar roles have also been suggested for UF-laser induced refractive index changes.^{10,11)}

Irrespective of the differing laser approaches, index changes in Fig. 2 shows similar orders of magnitude effects for both laser approaches. Accumulated fluence is one key control factor suggesting that total absorbed laser energy will define the index change. The F₂ laser induces an index change of 0.0001 to 0.0004 in pure fused silica for an accumulated fluence range of 3 to 30 kJ/cm². The response is improved more than 10-fold to $\Delta n = 0.005$ in germanium-doped fused silica, a much stronger absorber of 157-nm light. Similar index changes – $\Delta n = 0.001$ to 0.005 – are also noted for fused silica with the UF laser, whose light is fundamentally transparent to the material. The larger point-to-point scatter for the UF data (Fig. 2) is due to the sensitivity of NA measurements

to the waveguide quality. The UF-laser process is also intrinsically more sensitive to repetition rate, single-pulse fluence, and pulse number, and may therefore be more challenging to control unlike the F₂-laser approach.

Observed index changes in the range of $1\text{--}5 \times 10^{-3}$ are useful for a wide range of photonics manufacturing applications. An accumulated fluence of 20 kJ/cm² can be delivered rapidly for tightly focused UF laser sources, and form waveguides at scan speeds $\sim 1 \text{ mm/s}$ for high repetition rate systems. Excimer and F₂ lasers offer much higher power (10's W) than UF lasers ($< 1 \text{ W}$) and are therefore better suited to high volume applications, especially those where large area coverage is required such as in printing two-dimensional optical circuits. The UF laser is better suited to direct-write processing, a slower process, but one that offers more flexibility in patterning and trimming applications. The UF laser also has one substantial advantage over UV lasers – the internal structuring of three-dimensional index profiles in transparent glasses. This presents interesting prospects for shaping novel three-dimensional photonic structures for optical telecommunication applications. The fine control of index changes available from both laser classes will serve many niches as the current practice of UV-laser printing of fiber-based devices expands to two- and three-dimensional integrated structures.

6. Conclusions

Two extreme approaches in index profiling of transparent glasses have been examined in this paper. Deep-UV nanosecond lasers and 50-fs near-infrared laser light have been shown to induce index changes of 1 to 5×10^{-3} , a useful range for commercial purposes. The 157-nm F₂-laser offers strong photosensitivity responses in both fused silica and low-concentration germanosilicate glasses in comparison with traditional UV sources. UF lasers are another promising approach offering similar photosensitive responses. One key observation is that accumulated fluence is a common control parameter in both laser approaches. A total exposure of $\sim 20 \text{ kJ/cm}^2$ appears necessary to reach a $\sim 10^{-3}$ index change without damage to the glass structure. Such exposures are realizable in practical time frames, $\sim 100 \text{ ms}$ for the UF laser and several minutes for the UV laser. Both lasers – now commercially available – offer attractive prospects for shaping photonic components in fused silica and related glasses.

The authors gratefully acknowledge financial support from the National Research Council, the Natural Sciences and Engineering Research Council, Photonics Research Ontario, and the Canada Foundation for Photonics Innovation.

References

- 1) P. R. Herman, R. S. Marjoribanks, A. Oettl, K. Chen, I. Konovalov, and S. Ness: *Appl. Surf. Sci.* **154**, 577 (2000).
- 2) P. R. Herman, A. Oettl, K. P. Chen, and R. S. Marjoribanks: *Proc. SPIE* **3616**, 148 (1999).
- 3) P. R. Herman, K. P. Chen, P. Corkum, A. Naumov, S. Ng, and J. Zhang: *Proc. SPIE* **4088**, 345 (2000).
- 4) Raman Kashyap: *Fiber Bragg Gratings* (Academic Press, San Diego, 1999).
- 5) A. Othonos: *Review of Scientific Instruments* **68**, 4309 (1997).
- 6) K. Takada, T. Tanaka, M. Abe, T. Yanagisawa, M. Ishii, and

- K. Okamoto: *Electron. Lett.* **36**, 60 (2000).
- 7) J. Gehler and F. Knappe: *Opt. Fiber Comm. Conf. (OSA 2000)*, paper WM9-1.
 - 8) P. R. Herman, K. Beckley, and S. Ness: *Conf. on Lasers and Electro-Optics, Tech. Digest Ser.* **6**, 513 (1998).
 - 9) M. Rothschild, D. J. Ehrlich, and D. C. Shaver: *Appl. Phys. Lett.* **55**, 1276 (1989).
 - 10) D. C. Allan, C. Smith, N. F. Borrelli, and T. P. Seward III: *Opt. Lett.* **21**, 1960 (1996).
 - 11) K. M. Davis, N. Sugimoto, and K. Hirao: *Opt. Lett.* **21**, 1729 (1996).
 - 12) E. N. Glezer, M. Milosavljevic, L. Huang, R. J. Finlay, T.-H. Her, J. P. Callan, and E. Mazur: *Opt. Lett.* **21**, 2023 (1996); E. N. Glezer and E. Mazur: *Appl. Phys. Lett.* **71**, 882 (1997).
 - 13) D. Homoelle, S. Wielandy, A. L. Gaeta, N. F. Borrelli, and C. Smith: *Opt. Lett.* **24**, 1311 (1999).
 - 14) P. Lemaire, R. M. Atkins, V. Mizrahi, and W. A. Reed: *Electron. Lett.* **29**, 1191 (1993).
 - 15) J. Albert, B. Malo, K. O. Hill, F. Bilodeau, D. C. Johnson, and S. Theriault: *Appl. Phys. Lett.* **67**, 3529 (1995).